(12)

Report No. FAA-RD-75-123, I

IDENTIFICATION OF MINIMUM ACCEPTABLE CHARACTERISTICS FOR MANUAL STOL FLIGHT PATH CONTROL

Volume I. Summary

June 1976

Final Report

Document is available to the public through the National Technical Information Service, Springfield, Virginia 22161.

Prepared for

U.S. DEPARTMENT OF TRANSPORTATION
FEDERAL AVIATION ADMINISTRATION
Systems Research & Development Service
Washington, D.C. 20590

N O T I C E

TECHNICAL REPORT STANDARD TITLE PAGE

1. Report No. FAA-RD-75-123, I	2. Government Accession No.	3. Recipient's Catalog No. 11 12 47p.

4. Title and Subtitle (6)
Identification of Minimum Acceptable Characteristics for Manual STOL Flight Path Control, Volume I: Summary Report.

5. Report Date
June 1976

6. Performing Organization Code

7. Author(s) (10)
Roger H. Hoh, Samuel J. Craig and Irving L. Ashkenas

8. Performing Organization Report No.
(14) STI-TR-1035-3R-I

9. Performing Organization Name and Address
Systems Technology, Inc.
13766 S. Hawthorne Boulevard
Hawthorne, California 90250

10. Work Unit No.

11. Contract or Grant No.
(15) DOT-FA73WA-3276

12. Sponsoring Agency Name and Address
U.S. Department of Transportation
Federal Aviation Administration
Systems Research and Development Service
Washington, D.C. 20590

13. Type of Report and Period Covered
~~Summary Report~~ (9) Final rept.,

14. Sponsoring Agency Code

15. Supplementary Notes
(18) FAA-RD (19) 75-123-1

16. Abstract

Characteristics of powered lift STOL airplanes that lead to unacceptable flight path control for approach and landing are identified. Most of the findings are based on the results of a piloted ground based simulator program. However, a short variable stability flight test program was conducted to allow interpretation of the simulation landing results in light of a flight environment.

This report (Volume I) contains a comprehensive summary of the overall program including all of the significant results that were obtained. An important part of the research was an investigation of generic characteristics of various STOL concepts. This is reported in Volume II along with the generic STOL simulation model used in this program. Finally, Volume III contains the detailed analysis techniques used to analyze the experimental data. Also included in Volume III is a complete description of all the tested vehicles.

17. Key Words	18. Distribution Statement
Stability Control STOL Mathematical Model Flight Path	Document is available to the public through the National Technical Information Service, Springfield, Virginia 22161.

19. Security Classif. (of this report)	20. Security Classif. (of this page)	21. No. of Pages	22. Price
Unclassified	Unclassified	43	

340 425

METRIC CONVERSION FACTORS

Approximate Conversions to Metric Measures

Symbol	When You Know	Multiply by	To Find	Symbol
		LENGTH		
in	inches	*2.5	centimeters	cm
ft	feet	30	centimeters	cm
yd	yards	0.9	meters	m
mi	miles	1.6	kilometers	km
		AREA		
in^2	square inches	6.5	square centimeters	cm^2
ft^2	square feet	0.09	square meters	m^2
yd^2	square yards	0.8	square meters	m^2
mi^2	square miles	2.6	square kilometers	km^2
	acres	0.4	hectares	ha
		MASS (weight)		
oz	ounces	28	grams	g
lb	pounds	0.45	kilograms	kg
	short tons (2000 lb)	0.9	tonnes	t
		VOLUME		
tsp	teaspoons	5	milliliters	ml
Tbsp	tablespoons	15	milliliters	ml
fl oz	fluid ounces	30	milliliters	ml
c	cups	0.24	liters	l
pt	pints	0.47	liters	l
qt	quarts	0.95	liters	l
gal	gallons	3.8	liters	l
ft^3	cubic feet	0.03	cubic meters	m^3
yd^3	cubic yards	0.76	cubic meters	m^3
		TEMPERATURE (exact)		
°F	Fahrenheit temperature	5/9 (after subtracting 32)	Celsius temperature	°C

*1 in ≡ 2.54 (exactly). For other exact conversions and more detailed tables, see NBS Misc. Publ. 286, Units of Weights and Measures, Price $2.25, SD Catalog No. C13.10:286.

Approximate Conversions from Metric Measures

Symbol	When You Know	Multiply by	To Find	Symbol
		LENGTH		
mm	millimeters	0.04	inches	in
cm	centimeters	0.4	inches	in
m	meters	3.3	feet	ft
m	meters	1.1	yards	yd
km	kilometers	0.6	miles	mi
		AREA		
cm^2	square centimeters	0.16	square inches	in^2
m^2	square meters	1.2	square yards	yd^2
km^2	square kilometers	0.4	square miles	mi^2
ha	hectares (10,000 m^2)	2.5	acres	
		MASS (weight)		
g	grams	0.035	ounces	oz
kg	kilograms	2.2	pounds	lb
t	tonnes (1000 kg)	1.1	short tons	
		VOLUME		
ml	milliliters	0.03	fluid ounces	fl oz
l	liters	2.1	pints	pt
l	liters	1.06	quarts	qt
l	liters	0.26	gallons	gal
m^3	cubic meters	35	cubic feet	ft^3
m^3	cubic meters	1.3	cubic yards	yd^3
		TEMPERATURE (exact)		
°C	Celsius temperature	9/5 (then add 32)	Fahrenheit temperature	°F

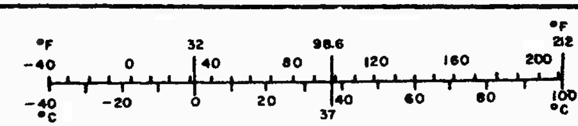

TABLE OF CONTENTS

LIST OF FIGURES

LIST OF TABLES

NOMENCLATURE

C_D	Drag coefficient
C_{D_α}	Drag curve slope
C_L	Lift coefficient
C_{L_α}	Lift curve slope
C_{L_o}	Lift coefficient at zero angle of attack
C_μ	Blowing coefficient, T/SQ
C_1, C_2	Constants (Eq. 2)
d	Deviation from glide slope; ft
d_ϵ	Glide slope error (equals −d when loop is closed as shown in Fig. 3); ft
g	Acceleration due to gravity; ft/sec^2
h	Perturbation altitude (change in altitude from trim); ft
K_1, K_2, K_3	Constants in Eq. 1
K_θ	Pitch-attitude-to-elevator feedback gain
$K_{\dot\theta}$	Pitch-rate-to-elevator feedback gain; sec
m	Mass of airplane
$N_{\delta_e}^{\theta}$	Numerator of transfer function which describes pitch-attitude-to-elevator response (see Ref. 2); becomes denominator of sink-rate-to-throttle response when attitude is constrained
$N_{\delta_e \delta_T}^{\theta \dot h}$	Coupling numerator due to closure of two loops to two different control points; becomes numerator of sink-rate-to-throttle response when attitude is constrained
Q	Dynamic pressure; lb/ft^2
S	Wing area; ft^2
t	Time; sec
T	Thrust; percent or lb

T_E	Pitch attitude SAS feedback time constant, $K_{\dot{\theta}}/K_{\theta}$; sec
T_F	Time constant for exponential flare; sec
$T_{h_{\theta}}$	Zero of coupling numerator, $N^{\theta\ \dot{h}}_{\delta_e\delta_T}$ (see Eq. 2a); sec
T_{h_1}	Zero of sink-rate-to-elevator numerator, $1/T_{h_1} = -g(\partial\gamma/\partial V)_{\delta_T}$
T_{pilot}	Compensation provided by pilot based on experimental measurements; sec
T_{θ_1}	Pitch attitude numerator ($N^{\theta}_{\delta_e}$) zero; speed mode time constant when pitch attitude is constrained (see Eq. 1); sec
T_{θ_2}	Pitch attitude numerator ($N^{\theta}_{\delta_e}$) zero; path mode time constant when pitch attitude is constrained (see Eq. 1); sec
u_g	Horizontal wind gust; ft/sec
U_o	Trim speed; ft/sec
w_g	Vertical wind gust; ft/sec
X_u	Equals $-(\rho SU_o/m)(C_D + C_{D_u})$; 1/sec
X_w	Equals $(\rho SU_o/m)(C_L - C_{D_\alpha})$; 1/sec
X_{δ_T}	Equals $-SQC_{D_{\delta_T}}$; (ft/sec^2)/percent
Y_p	Transfer function representing pilot control characteristics to a perceived error
Z_u	Equals $-(\rho SU_o/m)(C_L + C_{L_u})$; 1/sec
Z_w	Equals $-(\rho SU_o/2m)(C_D + C_{L_\alpha})$; 1/sec
Z_α	Equals U_oZ_w; (ft/sec^2)/rad
Z_{δ_T}	Equals $-SQC_{L_{\delta_T}}$
α	Angle of attack; deg or rad
γ	Flight path angle; angle of velocity vector with respect to horizontal
γ_{peak}	Maximum flight path response to a step throttle input
γ_{ss}	Steady-state flight path response after a step throttle input
δ_T	Percent power (throttle)
ζ_θ	See Eq. 2.

η_p	Powered-lift efficiency parameter; $-(\partial C_L/\partial C_\mu)(C_\mu/C_L)$
θ	Pitch attitude; deg or rad
θ_T	Effective thrust inclination angle; lumps aerodynamic and thrust effects into an equivalent thrust vector (θ_T = 90 deg when thrust is perpendicular to flight path); deg
ρ	Air density; slug-ft^2
σ_θ	Closed-loop bandwidth parameter (see Eq. 5)
ω_θ	Path mode frequency when pitch attitude is constrained (see Eq. 2)

SECTION I

INTRODUCTION

The purpose of this program has been to define characteristics or combinations of characteristics which result in minimally acceptable flight path control for powered-lift STOL airplanes. This summary report presents an overview of the results. Many of the results were obtained from closed-loop servo analyses considerations of the pilot/vehicle system. Wherever possible, these have been reinterpreted in terms of basic aerodynamic characteristics or time domain responses in this summary report.

A. PROGRAM SUMMARY

The research effort spanned a period of approximately two years and involved analysis, simulation, and flight test as outlined below.

- Definition of the generic properties of various STOL concepts with emphasis on those characteristics expected to result in minimally acceptable path control.
- Conduct of a two-phase simulation program with 11 generic STOL configurations and 9 pilots. Both phases of this simulation program were run on the NASA/Ames S-16 Moving-Base Simulator.
- Conduct of an abbreviated flight test program on the Princeton University Variable Stability NAVION to allow interpretation of the simulation final approach and landing results in light of a flight environment.
- Analysis of simulation results in terms of key parameters and critical flight path regimes defining minimum acceptable flight path control for powered-lift STOL vehicles.

B. DESCRIPTION OF GENERIC STOL CONFIGURATIONS

Eleven generic configurations were derived to characterize the extremes of potential variations in the performance parameters (C_L, C_D, and C_μ). The simulated airplanes are grouped and labeled in terms of their lift, drag, and thrust characteristics in Table 1. More specific descriptions of the variations of the performance parameters with thrust (C_μ) are given in Vol. III.

TABLE 1. SUMMARY OF CHARACTERISTICS OF THE SIMULATED CONFIGURATIONS

GROUP	CONFIGURATIONS	C_{L_o} VS. C_μ	C_{L_α} VS. C_μ	θ_T	REPRESENTATIVE STOL CONCEPT	COMMENTS
I	BSL1, 2, 2RLD	Linear and moderate	Linear and moderate	61 deg	Low efficiency EBJF or VT	BSL1 has 20% lower C_{L_α} than BSL2 and 2RLD. BSL2RLD has modified stall.
II	AP2, 6, 6RLD	Very non-linear	Nonlinear and moderate	90 deg	High efficiency IBJF	AP6 has improved $\Delta\gamma$ capability (-4 deg). AP6RLD has modified stall.
III	AP3, 7	Linear and moderately high	Nonlinear and moderate	75 deg	Low efficiency VT/MF or poorly designed EBJF	AP7 has improved $\Delta\gamma$ capability.
IV	AP1, 5	Linear and moderately high	Very low	81 deg	Low efficiency VT/MF	AP5 has improved $\Delta\gamma$ capability.
V	AP10	Very non-linear	Very low	90 deg	High efficiency EBJF	

The configurations were arbitrarily labeled BSL1 and 2 and AP1 through 10. The letters RLD following the configuration label stand for "rounded lift and drag" and indicate nonlinear lift characteristics at high angles of attack.

1. Steady-State Characteristics

The steady-state characteristics of the test configurations are summarized in terms of conventional γ-V contours in Fig. 1. A summary of the physical significance of the constant power and constant attitude lines in the γ-V plane is given in Vol. III.

2. Dynamic Characteristics

All of the tested configurations were flown using the backside technique, e.g., flight path was regulated with throttle. The time responses of sink rate to a step throttle change for each of the tested configurations are shown in Fig. 2. The Group I configurations (BSL1, BSL2, and BSL2 RLD) exhibit a somewhat sluggish path response. The Group III configuration (AP7) exhibits a slight overshoot and is more responsive to changes in throttle. Configurations AP1, AP2, and AP10 all exhibit significant path overshoot to a step throttle input. AP1 and AP2 are nearly identical in this regard. Some of the time response characteristics are summarized in Table 2.

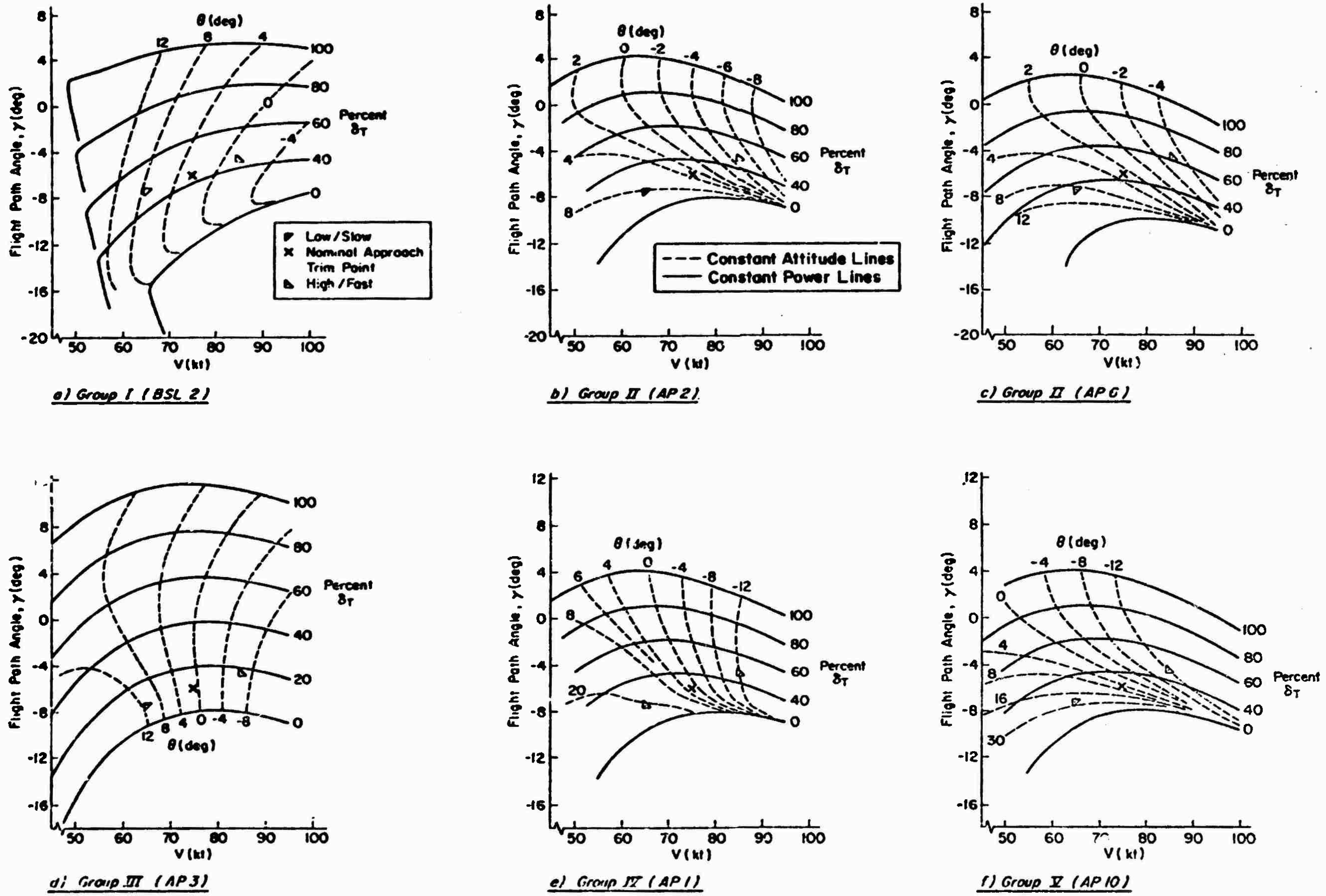

Figure 1. $\gamma - V - \theta$ Plots for the Tested Generic Configurations

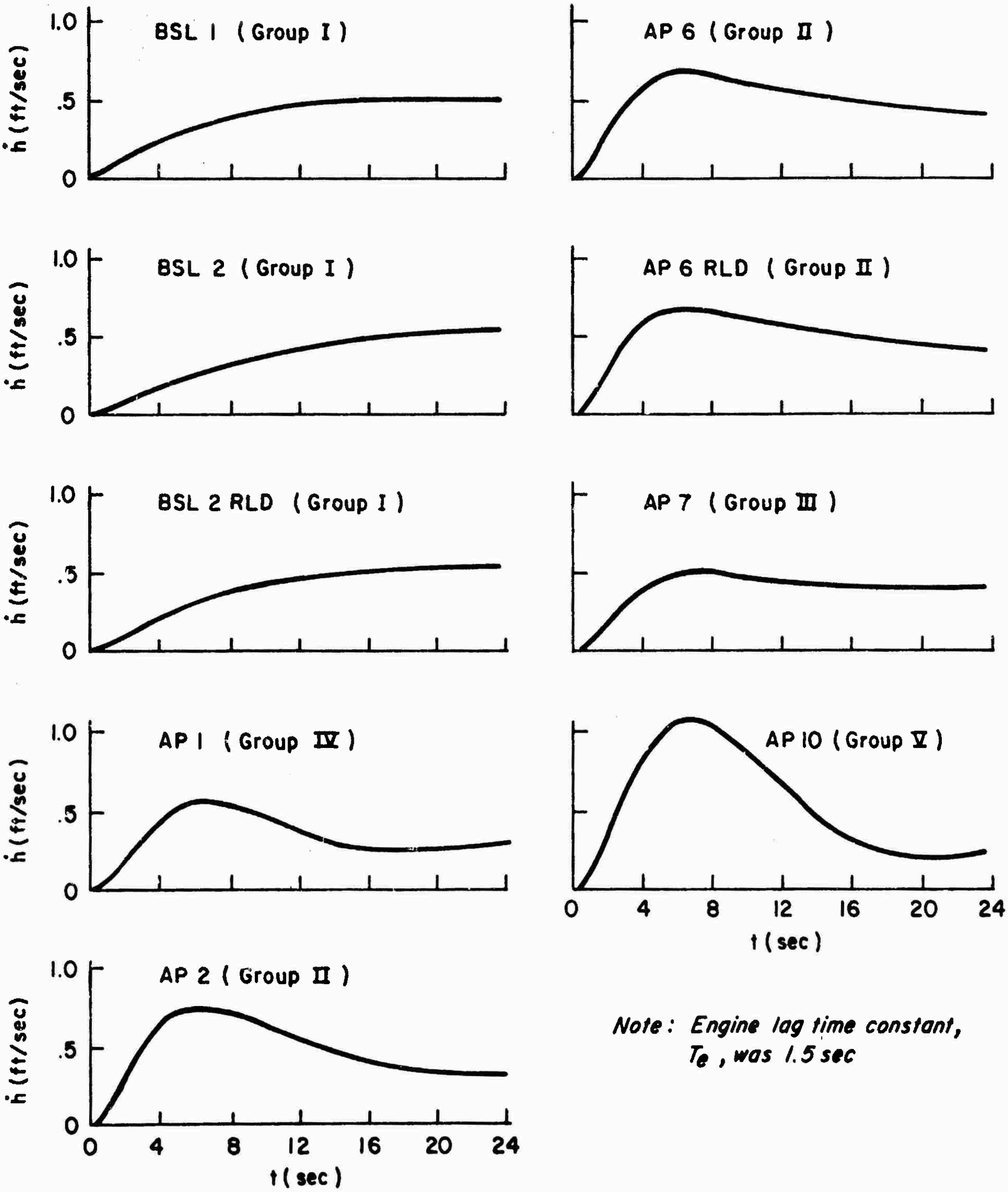

Figure 2. Time Responses to 1% Step Power Change (Attitude Constrained)

TABLE 2

SUMMARY OF TIME RESPONSE CHARACTERISTICS
OF TESTED CONFIGURATIONS

GROUP	CONFIGURATION	TIME TO 1/2 AMPLITUDE OF $\dot{h} \rightarrow \delta_T$ RESPONSE (FIG. 2), sec	$\gamma_{peak}/\gamma_{ss}$
I	BSL1	4.6	1.0
	BSL2	7	1.0
	BSL2 RLD	5	1.0
II	AP2	2.2	2.53
	AP6	2.1	1.72
	AP6 RLD	2.1	1.72
III	AP7	2.8	1.33
IV	AP1	2.6	1.93
V	AP10	2.7	4.40

The flight path to throttle dynamics can take on two separate characteristics depending on the values of certain vehicle aerodynamic and propulsive parameters. These are referred to as dynamically coupled and dynamically uncoupled responses, as illustrated generally by the following equations for sink rate to a step throttle input with pitch attitude constrained and zero engine lag.

- Dynamically uncoupled response:

$$\dot{h} \doteq K_1\delta_T\left[1 + \underbrace{K_2e^{-t/T_{\theta 1}}}_{\text{Speed Mode Response}} + \underbrace{K_3e^{-t/T_{\theta 2}}}_{\text{Path Mode Response}}\right] \tag{1}$$

or in terms of transfer function notation:

$$\dot{h} \doteq \frac{Z_{\delta_T}\delta_T(s + 1/T_{h_\theta})}{s\underbrace{\left(s + \frac{1}{T_{\theta 1}}\right)}_{\text{Speed Response}}\underbrace{\left(s + \frac{1}{T_{\theta 2}}\right)}_{\text{Path Response}}} = \frac{N^{\theta\ \dot{h}}_{\delta_e \delta_T} \leftarrow \text{Coupling Numerator}}{N^{\theta}_{\delta_e} \leftarrow \text{Attitude Numerator}} \tag{1a}$$

- Dynamically coupled response:

$$\dot{h} \doteq C_1\delta_T[1 + \underbrace{C_2 e^{-\zeta_\theta\omega_\theta t} \sin (\omega_\theta \sqrt{1-\zeta_\theta^2}\, t + \psi)}_{\substack{\text{Speed and Path Respond} \\ \text{Together at Frequency } \omega_\theta}}] \tag{2}$$

or in terms of transfer function notation:

$$\dot{h} = \frac{Z_{\delta_T}\delta_T(s + 1/T_{h_\theta})}{s(s^2 + 2\zeta_\theta\omega_\theta s + \omega_\theta^2)} = \frac{N^{\theta\,\dot{h}}_{\delta_e\delta_T} \leftarrow \text{Coupling Numerator}}{N^{\theta}_{\delta_e} \leftarrow \text{Attitude Numerator}} \tag{2a}$$

For conventional airplanes, the path and speed modes are dynamically uncoupled with path responding significantly faster than speed ($T_{\theta_2} << T_{\theta_1}$ in Eq. 1). Furthermore, conventional airplanes usually have a very low value of K_2 so that the speed response does not contaminate the sink rate response. Configurations which are dynamically coupled (Eq. 2) respond at the same frequency (ω_θ) in path and speed. The condition for dynamic coupling is:

$$(Z_w - X_u)^2 < -4X_wZ_u \tag{3}$$

This expression may be approximated in terms of the more basic nondimensional derivatives as follows:

$$C_{L_\alpha} < C_L\sqrt{8(1-\eta_p)(1 - C_{D_\alpha}/C_L)} \tag{3a}$$

where $\eta_p \doteq (\partial C_L/\partial C_\mu)(C_\mu/C_L)$. η_p is a measure of powered-lift efficiency (change in lift coefficient, C_L, with blowing coefficient C_μ).* Low values of η_p tend to result in dynamic coupling. Likewise, low values of lift curve slope, C_{L_α}, and drag curve slope, C_{D_α}, also tend to cause dynamic coupling. The tendency for dynamic coupling in powered-lift airplanes is due to very

*Actually, η_p arises directly from the change in lift coefficient with speed, e.g., $\eta_p \equiv C_{L_\mu}/C_L$. A more complete discussion of this parameter is given in Ref. 1, forthcoming.

large lift coefficients which more than offset η_p. To put things in perspective, η_p may be as large as 0.6, C_{D_α}/C_L is usually on the order of 0.6, and C_L was 4.8 for all of the generic configurations. The dynamic coupling properties of the tested configurations are summarized in Table 3.

TABLE 3

DYNAMIC COUPLING PROPERTIES OF TESTED CONFIGURATIONS

GROUP	TESTED CONFIGURATION	DYNAMIC COUPLING	$1/T_{\theta_1}$	$1/T_{\theta_2}$	ζ_θ	ω_θ
I	BSL1	Slight	—	—	0.93	0.30
	BSL2	No	0.15	0.54	—	—
	BSL2 RLD	Just Barely	—	—	1.0	0.29
II	AP2	No	0.21	0.35	—	—
	AP6	No	0.11	0.50	—	—
	AP6 RLD	No	0.12	0.50	—	—
III	AP7	Yes	—	—	0.81	0.33
IV	AP1	Yes	—	—	0.52	0.32
V	AP10	Yes	—	—	0.59	0.27

C. PILOTING TASKS

The generic configurations described in Tables 1, 2, and 3 were evaluated in a comprehensive simulation program on the NASA Ames S-16 simulator. A summary of the piloting tasks is given in Table 4.

TABLE 4

SIMULATION TASK DESIGNATION AND DESCRIPTION

TASK DESIGNATION	TASK DESCRIPTION
	Glide slope tracking (Start at 1100 ft and terminate at 300 ft of altitude -- all IFR)
1.0	Calm air
1.01	Turbulence (σ = 4.5 ft/sec) (IFR only)
1.1	High fast initial condition (IFR only)
1.2	Low slow initial condition (IFR only)
1.7	Speed change on glide slope (IFR only)
	Landing (Initial condition at 300 ft — VFR)
2.0	Attitude flares and power flares in calm air
2.1	Add turbulence (σ = 4.5 ft/sec)
2.7	Add discrete shear
	Composite ILS approach task (Rate glide slope intercept, path control, and flare and landing separately)
3.0	Calm air (IFR and VFR)
3.1	Turbulence (σ = 4.5 ft/sec) (IFR and VFR)
3.2	Headwind (IFR and VFR)
3.3	Tailwind (IFR and VFR)

SECTION II

GLIDE PATH CONTROL RESULTS

The results of the glide path tracking tests showed that ILS glide path control was not the critical feature of the total approach and landing problem. Even though the experimental matrix included some configurations with apparent drastic deficiencies (low path damping, large path/speed coupling, very sluggish response, large engine lag), the pilot ratings and commentary indicated little differences among the configurations. None of the configurations was rated as unacceptable for the IFR ILS tracking task down to 300 ft (task was terminated at breakout). When this task was extended to include the visual portion of the approach down to flare, significant degradations in the pilot ratings were observed to occur for some configurations. A comparison of pilot ratings for the IFR only task (ILS) and the task which included visual tracking to the flare point (ILS plus visual) is shown in Fig. 3. Configurations AP1 and AP10 are seen to exhibit increased numerical pilot ratings along with increased rating variability which is symptomatic of inconsistent run-to-run performance with degraded configurations.

Evidence that the degraded pilot opinion ratings in Fig. 3 are directly attributable to the final portion of the approach is quite conclusive from the associated pilot commentary which is summarized in Table 5. The <u>key result</u> here is that the most critical portion of an ILS approach and landing with a marginal or unacceptable aircraft is the visual tracking on <u>short final</u>. Those features of the tracking task on short final which appear to contribute most heavily to its critical features (most commonly commented on by the pilots) are summarized below:

- The effects of path disturbances due to turbulence and shear were very prominent due to the near proximity to the ground.
- The terminal control nature of the task required that errors (in the apparent touchdown aim point) be eliminated immediately which is synonymous with the need for a highly responsive (i.e., high bandwidth) controlled element. This sense of urgency does not exist in the ILS task.
- The short STOL runway leaves very little margin for error in setting up for the flare.

TABLE 5. PILOT COMMENTARY WHERE FLIGHT PATH CONTROL PROBLEMS ON SHORT FINAL WERE SPECIFICALLY NOTED (TASKS 2.1 AND 3.1)

	PILOT 1	PILOT 2	PILOT 3	PILOT 7	PILOT 8	PILOT 9
BSL1	None	Poor vertical speed response makes it easy to overcontrol Put on too much power to correct for a low condition and then don't get it off in time, etc.		None	None	Am flying glide slope (ILS) to get to window for flare
BSL2	None	None		I am having quite a bit of problems with the turbulence particularly during the final glide slope tracking and the flare	None	None
BSL2RLD	Requires moderate compensation on throttles to set up for flare			None		Poor sink rate to throttle response is responsible for problems in getting set up at flare point Flying IVSI to throttles even in close
AP1	The primary deficiency is a very sluggish sink rate to throttle response. The major problem is the inability to recover from off nominal vertical position in time to set up for landing on this short runway		Pilot rating is a 3 down to breakout and then a 7 on short final	The workload gets too high trying to get the power set for your flare, particularly with these last minute flight path corrections where the power can be going up and down	... real dicey to get a good sink rate and a good aim point on the runway	Primary difficulty was the considerable lag in the throttle and if your effecting a change on glide path the resulting change in sink rate late in the approach will give you reel problems
AP2	The primary problem in landing is setting up for the flare with power in the presence of these fairly large gust disturbances	Recovery from turbulence effects coming into the flare was difficult		Turbulence is not a problem and getting set up for flare is also not a problem with this configuration		
AP5	None	None		None		
AP5RLD	Moderate compensation on sink rate control with power is required to set up the flare point			Sink rate response to attitude and power are good		None
AP7	None			None		None
AP10	The sluggish sink rate to throttle makes it difficult to get set up. My primary objection to this configuration lies in the inability to control sink rate during the last several hundred feet of the approach			The main problem with flight path control is that flight path angle washes out after a throttle input. This problem is especially noticeable as you approach the flare point and even during the flare	Got low and slow, a bear to correct	Seems very sensitive to throttle making it difficult to set up for flares. Extremely hard to get into proper flare window

Notes: Blank space means pilot did not fly the configuration.
"None" means that no specific comments relative to flight path control on short final were recorded.

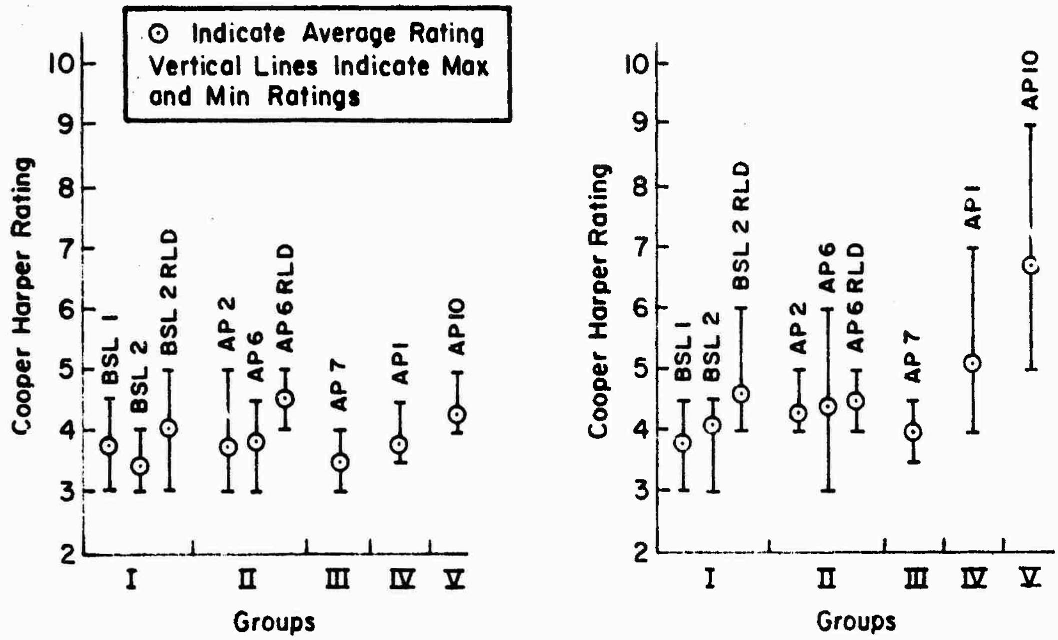

a) Pilot Rating for Glideslope Tracking Task (1.01) (IFR Only)

b) Pilot Ratings for Path Control Part of Composite Task (3.1) (IFR and VFR Path Control)

Figure 3. Pilot Ratings for Path Control

The commentary in Table 5 represents conclusive evidence of significant flight path control problems in that all the pilots who flew AP1 (and AP10) noted serious deficiencies on short final. The final conclusion that AP1 and AP10 were less than minimally acceptable for flight path control was based as much on the commentary as on the ratings in Fig. 3b.

A review of the comments for AP1 and AP10 in Table 5 reveals that the pilots had a very difficult time trying to sort out what the actual problem was. Some said that the response was sluggish, probably referring to the fact that the longer-term flight path correction was a lot less than indicated from the initial response. The engine lag was decreased from the nominal 1.5 sec to 0.5 sec for several pilots. All indicated that they could see the effect, but it was of no help in controlling flight path for these two configurations. (There was no change in pilot rating.) This served as evidence that the pilots were not referring to engine lag effects when commenting on the excessively "sluggish" response of AP1 and AP10.

Utilizing closed-loop pilot/vehicle analysis procedures, it was determined that the flight path control problems associated with AP1 and AP10 were due to a combination of severe dynamic coupling (see Table 3) and a large effective thrust inclination angle (see Table 1). These results arose directly from frequency response considerations and are felt to be important enough to include (briefly) in this summary report.

The fundamental closed-loop piloting problem was analyzed using the frequency response characteristics of the sink rate, $\dot{h}$, to throttle, δ_T, transfer functions plotted in Fig. 4 for AP1 (a bad configuration) and AP2 (a good configuration). Utilizing experimental and theoretical results from the theory of manual control (for example, see Ref. 2), it can be shown that the flat region in the frequency response (for AP1) represents a fundamental limitation on closed-loop control. This stems from the fact that the human operator <u>always</u> tries to adjust his control inputs so as to equalize the vehicle frequency response to a −20 dB/decade slope (or K/s shape). With mid-frequency droop, this was not possible.* (See Section IV-C of Vol. III for experimental evidence of this result.) Faced with undesirable and non-equalizable response characteristics, the pilots rated these configurations very poorly. Physically this was manifested in a path response to throttle that initially looked very good, but never seemed to settle down. As a result, the pilots were "constantly hunting for the proper throttle setting as they came into the flare."

The primary purpose of this program was to identify vehicle characteristics which result in unacceptable path control. Comparison of the time response and frequency response characteristics of AP1 and AP2 in Fig. 4 reveals the following:

- The shape of the time responses is about the same.
- The shape of the frequency responses (including pilot lead) is noticeably different. AP2 is almost a pure −20 dB/decade slope (desirable K/s feature) whereas AP1 has a significant mid-frequency droop (undesirable and unequalizable by the pilot).

---

*It should be noted that an automatic system could be developed with complex equalization to get an acceptable response but that this is beyond the capability of the human pilot.

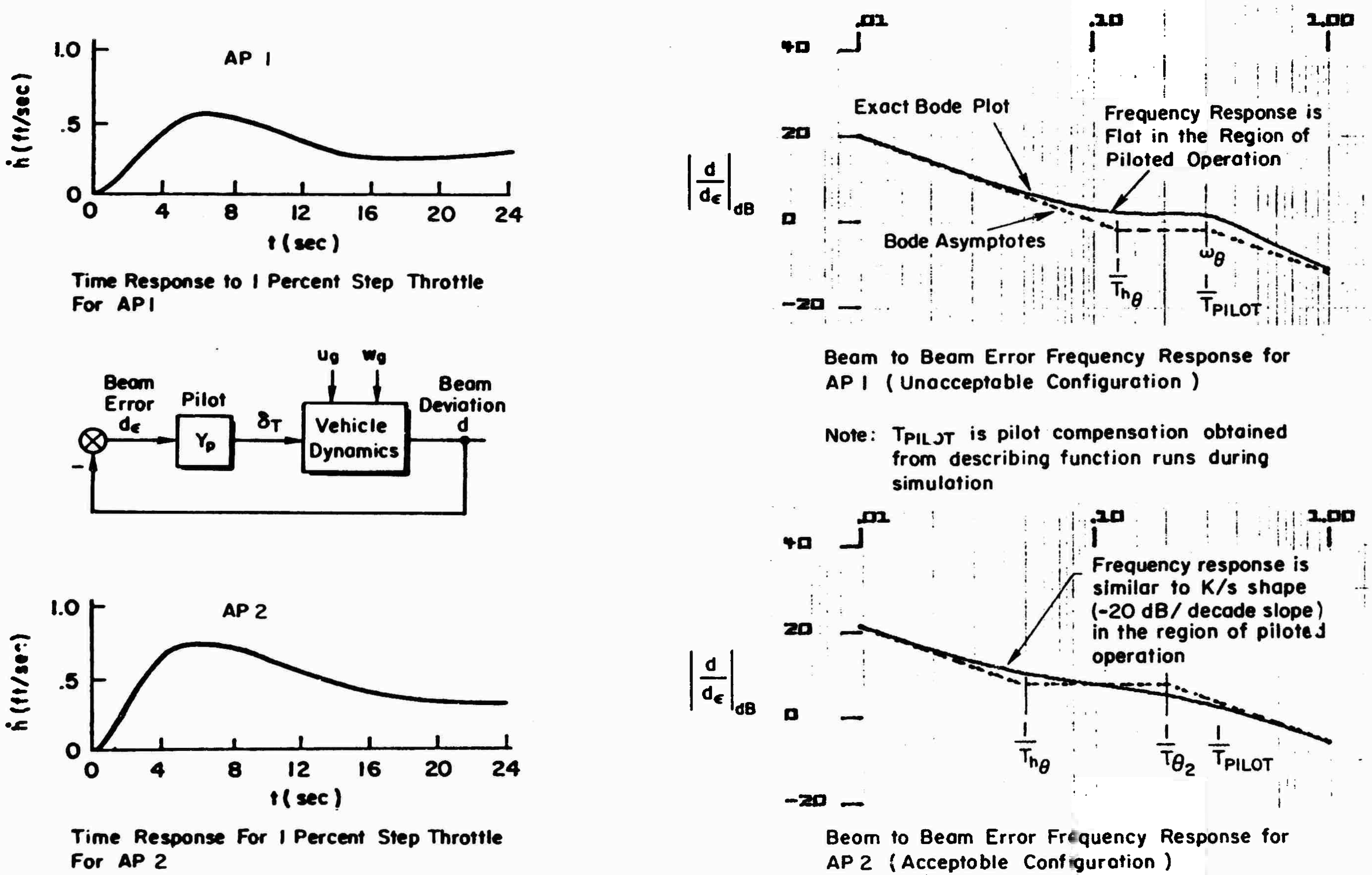

Figure 4. Time and Frequency Response Characteristics of an Acceptable and an Unacceptable Configuration

The pilot ratings (Fig. 3) and commentary (Table 5) strongly indicate that AP1 is unacceptable and AP2 is acceptable. Therefore, it appears that the frequency response characteristics are more discriminatory in terms of identifying limiting path control deficiencies. Consideration of the frequency response plots for AP1 and AP10 reveals that the limiting mid-frequency droop condition tends to occur when both of the following conditions are satisfied:

1. The configuration must be dynamically coupled, e.g., the denominator of the sink-rate-to-throttle transfer function, $\dot{h}/\delta_T$, is a complex pair. Note that AP1 is highly coupled and AP2 is uncoupled (see Eq. 3 and Table 3).

2. The $\dot{h}/\delta_T$ numerator zero ($1/T_{h_\theta}$) is much less than ω_θ ($1/T_{h_\theta} \ll \omega_\theta$). This gives the flat region or "shelf" in the Bode plot for AP1 in Fig. 4. It occurs when the thrust inclination angle is nearly vertical (greater than 75 to 80 deg).

The above results indicate that unacceptable flight path control results from a combination of two effects: large thrust inclination angle and dynamic coupling. From Eq. 3a the latter stems from low lift curve slope (C_{L_α}), low STOL efficiency (η_p), and low C_{D_α}. By definition, efficient powered-lift designs must have a large (near 90 deg) effective thrust inclination angle. It is therefore essential that dynamic coupling be avoided in these airplanes. Fortunately, some pretty extreme (but not inconceivable) values of C_{L_α} and C_{D_α} were required to get the path and speed modes dynamically coupled in AP1 and AP10. [C_{L_α} = 4.6 (1/rad) and C_{D_α} = 0.737 (1/rad), whereas more "typical" values are C_{L_α} = 7 (1/rad) and C_{D_α} = 2 (1/rad).]

While there are not sufficient data to allow definition of exact boundaries where flight path control becomes less than minimally acceptable, we can observe that AP1 is essentially on the boundary with pilot ratings between 4 and 7. AP1 had a thrust inclination angle of 81 deg and was quite heavily coupled ($\zeta_\theta = 0.52$; see Table 3).

The above results should not be construed to mean that decreasing the thrust inclination angle (thereby increasing $1/T_{h_\theta}$) would automatically fix an unacceptable configuration. One must also consider path control limitations arising from an overly sluggish response which could occur if $1/T_{h_\theta} \gg \omega_\theta$ and ω_θ was low.

A. EFFECT OF STEADY-STATE PATH/SPEED COUPLING

Path and speed are said to be statically coupled when a change in power intended to change flight path results in a new trim (steady-state) airspeed (attitude fixed). Conventional airplanes are said to be proversely coupled because increasing power results in an increase in path angle and speed. Adverse steady-state path/speed coupling refers to the case where an airplane loses airspeed when flight path is shallowed by increasing power. From Fig. 1 it can be seen that the Group I airplanes were proversely coupled, Group III was neutral, Group IV had weak-to-moderate adverse coupling, and Groups II and V were severely adversely coupled. There is a considerable body of experimental evidence that adverse path/speed coupling is a heavy contributor towards the definition of minimum acceptable boundaries (for example, see Refs. 3, 4, and 5). This was not the case for the configurations tested in this experiment. While the pilots found that adverse speed/path coupling was undesirable, it was not a major factor in the final pilot ratings. The evidence upon which this conclusion is based in summarized below.

- Quantitative measurements of the pilot's closed-loop tracking behavior via describing functions showed no evidence of active (closed-loop) speed control (these measurements are discussed in Vol. III).

- A review of the pilot commentary indicated that speed was monitored rather than controlled for adverse coupled configurations. Additionally, some pilots volunteered that the adverse speed/path coupling represented a rating degradation of only 1/2 to 1 point.

- The strip chart records from the simulation show evidence of changes in trim pitch attitude with long-term speed excursions but no evidence of closed-loop speed control. This result holds true for the IFR glide slope tracking portion of the approach, as well as the visual aim point control after breakout and before the initiation of flare. The pilots' apparent lack of concern over adverse path/speed coupling was based on the fact that, for the tested configurations, safety and performance margins did not depend on airspeed. A single exception to this was AP6 RLD. The pilot rating for Configuration AP6 RLD was initially a 9. This rating was given after a run where the pilot got low on short final and added power. Because of the strong adverse coupling on this configuration, the airspeed decreased to below stall and control was lost (too low to recover). The stall speed was decreased slightly (64 kt to 61 kt) so that increasing power at the trim pitch attitude did not result in a stall (increased $C_{L_{max}}$ by 10 percent) as shown in Fig. 5. The pilot rating then improved to a 5.

In summary, the above results indicate that as long as the flight path response or aircraft safety margins were not degraded, the pilots tended to simply monitor speed and fly constant attitude. Adverse speed/path coupling had only a minimal effect on the pilot ratings, which tended to be more directly associated with ability to control the flight path itself. These results were published in early progress reports and were checked by other investigators running STOL certification programs (Ref. 5). These investigators concurred that the pilots were not controlling airspeed for adversely coupled configurations.

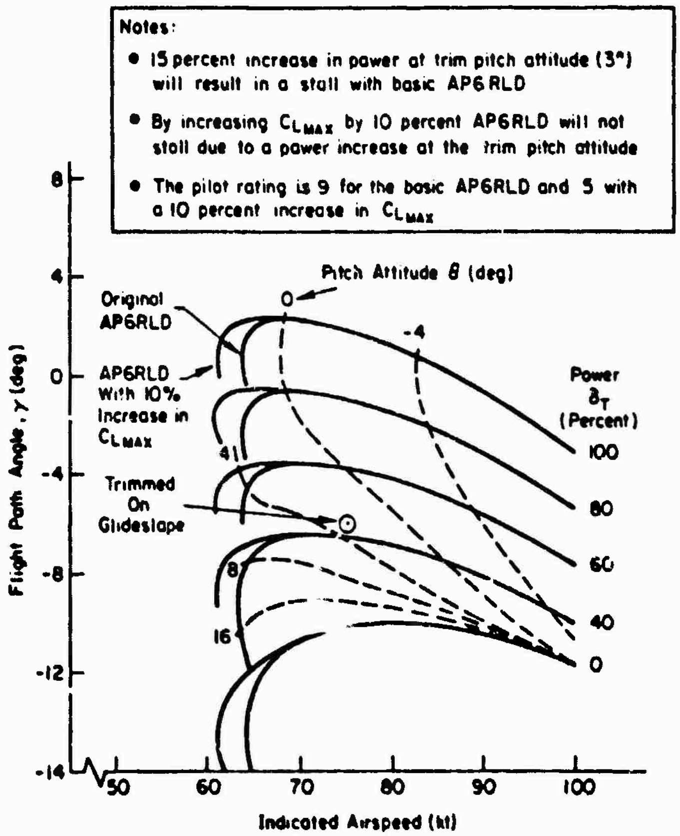

Figure 5. Effect of 10 Percent Increase in $C_{L_{max}}$ on Stall Characteristics

The stall problem discussed above is not the only safety margin that can be adversely affected by adverse steady-state path/speed coupling. As an example of a safety margin that would be affected by poor speed control consider the excess flight path capability variation with airspeed of some typical powered-lift airplanes (see Fig. 6). On many current STOL designs, the flight path performance in the up direction (γ_{max} at 100 percent power) is somewhat less than on the test configurations in this experiment. For these configurations, adverse static path/speed coupling would mean an even lower γ_{max} when thrust is added at constant attitude (see Fig. 6) due to reduced speed. Because of the adverse path/speed coupling, the likelihood of experiencing low speeds (and hence lower γ_{max}) is very high. Thus, we must consider safety margins other than stall when evaluating the effect of adverse path/speed coupling.

One other possibly limiting deficiency with large adverse path/speed coupling was noted briefly during the variable stability flight test portion of the program. This occurred when several approaches were made in a tailwind which sheared to a slight headwind near touchdown. The configuration being tested was AP1 which has light-to-moderate adverse steady-state path/speed coupling (see Fig. 1e). Because of the reduced power required to maintain glide slope in a tailwind, the airspeed tended to be quite high coming into the flare (90 kt or 15 kt above the target speed), making it difficult

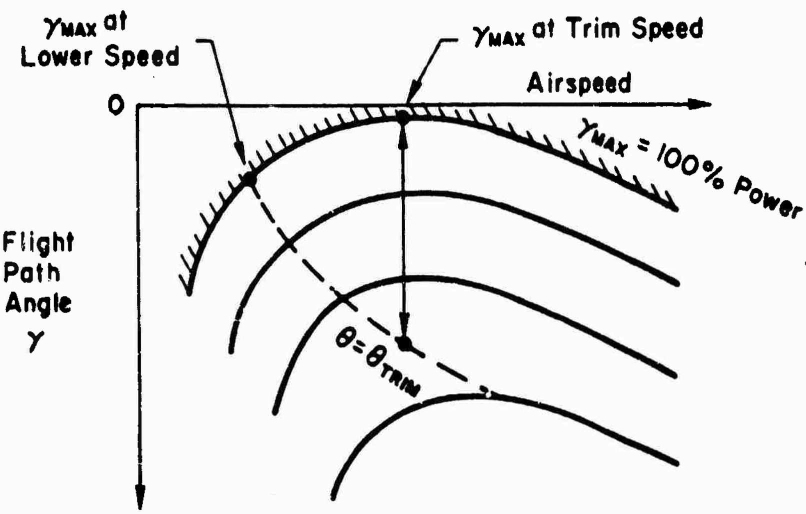

Figure 6. Illustration of Effect of Speed on Maximum Achievable Flight Path Angle

to get into the touchdown zone. Several approaches were made with increased pitch attitude to keep the airspeed within reason coming into the flare. This was entirely unsuccessful because it left no pitch attitude for the flare itself. Flares with power (pitch attitude held constant) were unsuccessful because of the very large engine lag (T_E = 1.5 sec) used in the experiment. The effect of a tailwind on final approach should be carefully considered when evaluating STOL configurations with adverse static path/speed coupling.

B. FLIGHT DIRECTOR RESULTS

Two flight director configurations were designed to provide the pilot with command information for column, throttle, and lateral wheel inputs. The flight directors were designed to be compatible with the Group I and Group II configurations using the STOL flight director design procedures developed in Ref. 6. The primary objectives of the flight directors were to reduce the pilots' workload and to increase glide slope and localizer tracking accuracy. In keeping with these objectives the guidance and control and pilot-centered requirements discussed in Ref. 6 were a primary factor in formulating the appropriate feedback signals for the flight directors. A third objective was to investigate the flight director as a means of decoupling the airspeed flight path responses. It was hypothesized that with a good flight director the displayed quantities can be quite well decoupled with regard to pilot inputs even though the basic airplane responses (airspeed and flight path) are quite highly coupled. The basic loop structures for the column and throttle flight director were taken directly from Ref. 6.

The directors were based on the principle of normal "backside" or STOL operation, i.e., throttle controls path deviations and attitude controls speed. The column flight director was basically an attitude hold with a low gain speed feedback [$\Delta\theta/\Delta V \doteq (0.34$ deg/kt$)$]. The speed error limiter was set to ±29.6 kt which results in a maximum flight director pitch command of ±10 deg. Attempts to increase the speed feedback gain and/or open up the speed error limiter met with unfavorable pilot commentary. This was primarily due to the increased activity of the pitch command bar. These results are consistent with the concept that the feedbacks to each of the controls must be frequency separated. That is, one control is primary (glide slope to throttle) and the other is a low frequency trim function (airspeed to attitude). We therefore may conclude that the flight director is effective in decoupling the aircraft responses only from the standpoint that one variable (speed in this case) is controlled very loosely. This is entirely consistent with the way the pilots flew the aircraft using "raw data" glide slope information.

A few of the pilots felt that the workload required to keep all three director commands centered was excessive. Their initial ratings were unacceptable. However, when instructed to fly the director commands "more loosely" the comments and ratings moved into the acceptable range. These pilots never were totally convinced, as evidenced by such comments as "the performance was excellent but the workload was a little higher than with raw data." Other pilots felt that the flight director resulted in a considerable improvement in workload level and performance.

The pilot ratings and ILS tracking performance results are summarized in Fig. 7 to show comparisons with and without the flight director in turbulence. These results show that:

- The flight director improves the pilot rating 1 to 1-1/2 points. In terms of Cooper Harper descriptors this implies "moderate to extensive compensation" with raw data to "minimal compensation" with the flight director.
- Averaged rms glide slope tracking performance was improved 25 to 40 percent with the flight director.
- Averaged rms localizer tracking showed the most dramatic improvement in performance (up to 86 percent reduction in rms tracking error).

C. SUMMARY OF GLIDE PATH CONTROL RESULTS

The glide path control results are summarized below.

- Major deficiencies in path control were found to be most apparent during short final and in the landing flare. IFR glide slope tracking was not found to be critical for any of the configurations.

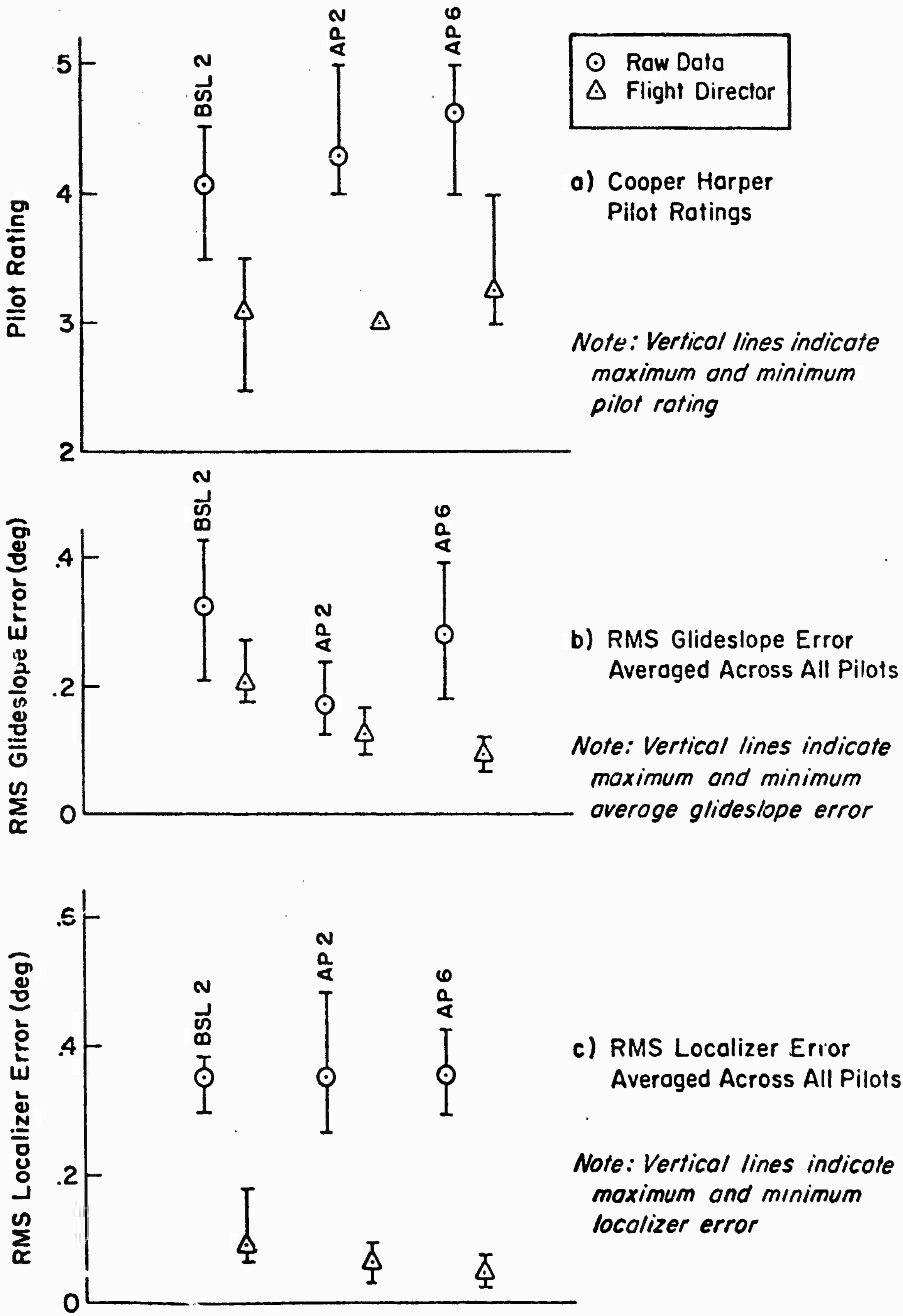

Figure 7. Effect of Flight Director on Ratings and Performance

- Unacceptable flight path control resulted from a combination of two effects: near vertical thrust inclination angle; and dynamic coupling (when the roots of the attitude-to-elevator numerator are a complex pair, see Eqs. 1-3). The latter effect tends to occur when the life curve slope C_{L_α} is low, the drag curve slope is low, and the STOL efficiency η_p is low (see Eq. 3).

- Adverse static flight-path/airspeed coupling was found to be undesirable by the pilots but not a dominant factor in the ratings (which were found to be more directly associated with ability to control flight path). Flight-path/airspeed coupling would, of course, be a limiting factor if it led to other problems such as regions of degraded path control or safety limits (such as stall). A problem with adverse coupling was briefly noted during the flight program in a tailwind (shearing to a headwind). This should be further investigated as it may represent a limiting path control item.

- The addition of a flight director tended to improve the pilot ratings and performance. It did not, however, allow the pilots to decouple the path and speed responses for aircraft with significant path/speed coupling. The most significant effect of the flight director was on the lateral lineup at breakout, and this resulted in drastically improved performance. Some pilots noted that while their performance was significantly improved by the flight director, the workload was also correspondingly increased. This was due to the intense concentration required to keep three needles centered (glide slope, localizer, and throttle directors) while still maintaining some awareness of the status information.

SECTION III

FLARE AND LANDING RESULTS

Atmospheric turbulence had a very strong adverse effect on pilot opinion ratings and performance for the final approach and landing. As shown in Fig. 8, Configurations BSL1, BSL2 RLD, AP7, and AP1 were particularly sensitive to turbulence.

Closed-loop servo analysis techniques were utilized to identify certain key parameters which define the dominant pilot/vehicle characteristics in the flare maneuver. These parameters were then compared with experimentally derived pilot ratings in an attempt to achieve correlations, and when successful, to approximate the shapes and values of the limiting boundaries. The basic hypothesis of this analysis was that the pilot must be able to break the sink rate without using excessive pitch attitudes, and he must be able to precisely regulate sink rate in a closed-loop fashion. For flares where pitch attitude was the primary control (conventional) the following parameters were derived (see Vol. III):

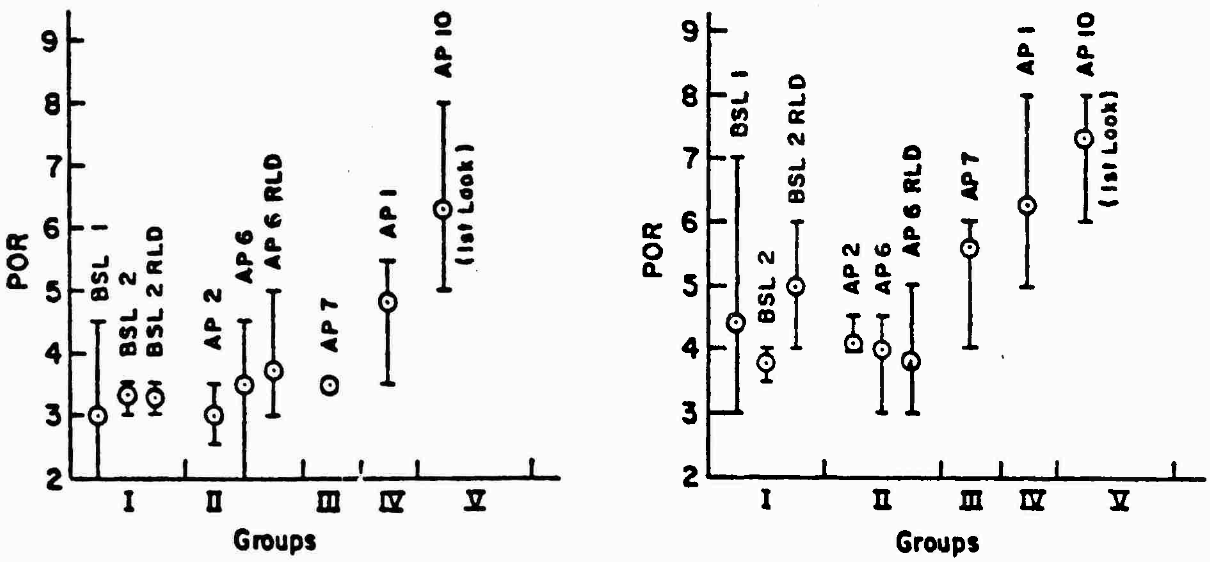

a) Pilot Ratings for Final Approach and Landing Task (2.0); $\sigma_{u_g} = 0$

b) Pilot Ratings for Final Approach and Landing Task (2.1); σ_{u_g} = 4.5 ft/sec

Figure 8. Pilot Ratings for Approach and Landing Task

- Magnitude of pitch attitude required to break sink rate

$$\frac{\theta}{\dot{h}_o} = \frac{1}{T_F U_o Z_w} = \frac{1}{T_F Z_\alpha} \tag{4}$$

- Closed-loop regulation parameter

$$\sigma_\theta = \zeta_\theta \omega_\theta + \frac{1}{2}\left(\frac{1}{T_E} - \frac{1}{T_{h_1}} - \frac{1}{T_F}\right)$$

or, very approximately

$$\sigma_\theta \doteq Z_w + \frac{1}{2}\left(\frac{1}{T_E} - \frac{1}{T_F}\right) \tag{5}$$

where $\zeta_\theta \omega_\theta$ is the coefficient of s in the numerator of the pitch-attitude-to-elevator transfer function. $1/T_E$ is the feedback compensation in the attitude SAS ($T_E = K_{\dot{\theta}}/K_\theta$) and T_F is defined by the flare geometry and varies from 2.5 to 5 sec for STOL landings. The above parameters indicate that the magnitude of the required pitch attitude in the flare depends on the product of speed and Z_w ($U_o Z_w = Z_\alpha$), whereas the closed-loop regulation capability depends on Z_w alone.

We therefore expect that configurations with very low Z_α would require excessive pitch attitude to break the sink rate in the flare. The only alternative in these cases would be to revert to power as a secondary control in the flare. Such a technique was evolved by the pilots and consisted of an initial power increase to break the sink rate followed by fine tuning the touchdown with pitch attitude. These were termed "combination flares" (power and attitude). Pure power flares were not possible because of the very large engine lag (T_E = 1.5 sec) utilized in the experiment. The pilots were asked to try all three flare techniques (pure attitude, pure power, and combination) during the familiarization runs and to state their preference at the end of the simulation test period (familiarization and formal runs). The results are shown in Fig. 9 where it is seen that there was a narrow range of Z_α where the appropriate flare technique was uncertain, e.g., between 50 and 60 (ft/sec^2)/rad. For values of Z_α at or less than about 55 most of the pilots found that an initial power input was necessary to break the sink rate so that the nose would be low enough to allow the final touchdown to be

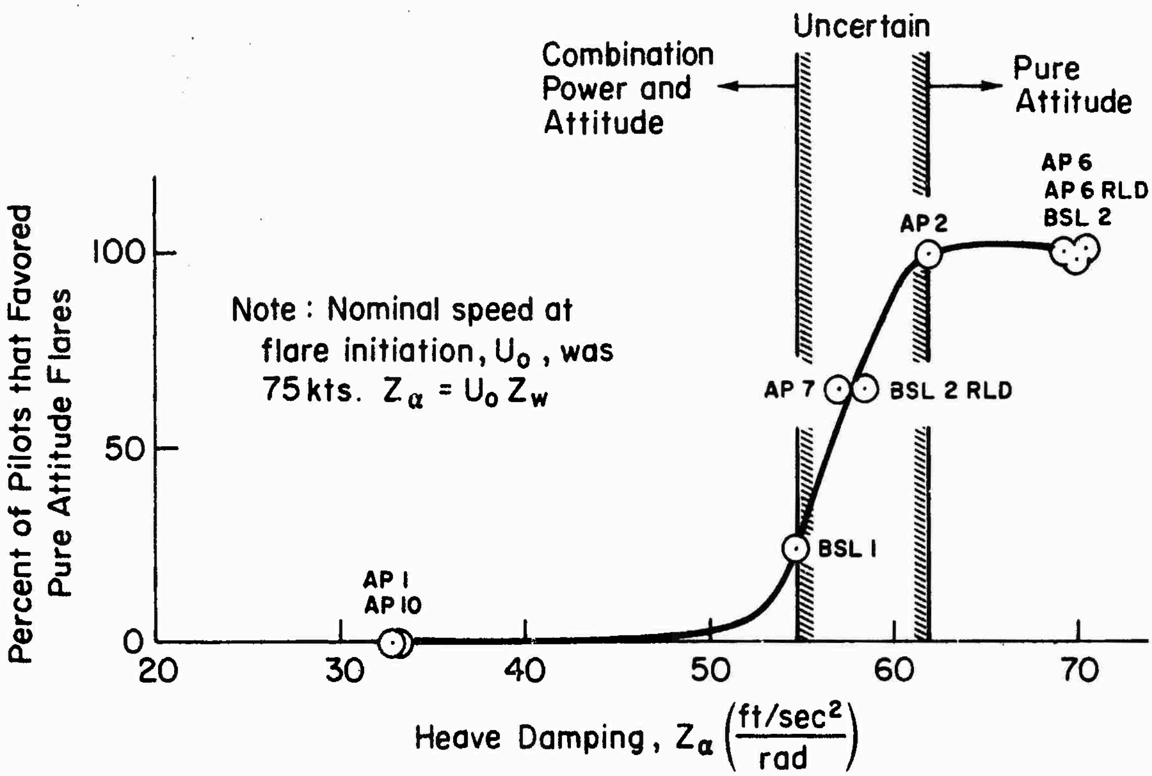

Figure 9. Experimental Results of Pilots' Control Technique for Flaring

more precisely adjusted with attitude. Based on Fig. 9, there was sufficient authority to complete the entire flare maneuver with attitude when Z_α exceeded about 60.

As discussed earlier (Eq. 5), the ability to achieve good closed-loop regulation of sink rate with pitch attitude was related to the closed-loop bandwidth parameter σ_θ. It can also be shown via closed-loop pilot/vehicle analysis that the propensity of a configuration to be perturbed vertically due to a horizontal gust or wind shear depends primarily on the derivative Z_u. For conventional aircraft in subsonic flight, Z_u is simply a function of the trim lift coefficient:

$$Z_u \equiv -\frac{\rho S U_o}{2m} C_L$$

For steady flight where lift equals weight this may be very closely approximated as:

$$Z_u = -\frac{2g}{U_o}$$

For powered-lift STOL configurations, Z_u is modified as follows:

$$Z_u = -\frac{2g}{U_o}(1 - \eta_p)$$

where

$$\eta_p = \frac{\partial C_L}{\partial C_\mu}\frac{C_\mu}{C_L} \tag{6}$$

$\partial C_L/\partial C_\mu$ is the change in lift coefficient with blowing coefficient (power) and is therefore a measure of the efficiency of the powered-lift concept. For efficient STOL concepts, η_p may vary from 0.2 to 0.6, thereby lowering the gust sensitivity a moderate amount (20-60 percent).

A logical set of correlating parameters would therefore be Z_u (tendency to be disturbed from the desired path) versus σ_θ (ability to quickly return to the desired path). Figure 10 presents σ_θ versus Z_u for the configurations tested in the present experiment.

Referring to Fig. 10, certain trends in the experimental results (pilot ratings) may be explained as follows:

- AP1 and AP10 were rated unacceptable because σ_θ (a measure of piloted closed-loop regulation of sink rate with attitude) was too low.

- The value of σ_θ for Configurations BSL1, BSL2 RLD, AP2, AP6, AP6 RLD, and AP7 are all about the same (σ_θ = 0.5 to 0.55). From Fig. 10 it is seen that this value of σ_θ is acceptable for configurations with low gust sensitivity (Z_u). However, as the gust sensitivity is increased to approximately the CTOL value ($Z_u \doteq -2g/U_o$), the pilot ratings begin to degrade into the unacceptable region (BSL1, BSL2 RLD, and AP7).

These results are not conclusive in that the poor ratings could have been either wholly or in part due to unacceptable secondary control (throttle)

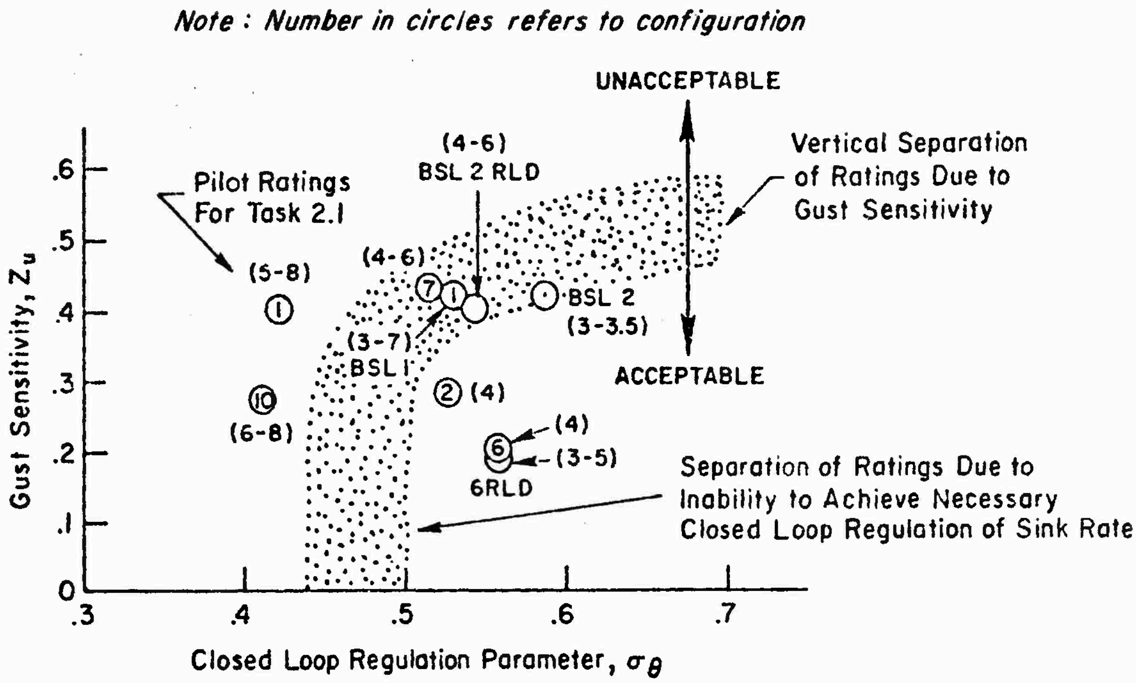

Figure 10. One Possible Way of Using Key Parameters to Correlate Minimum Acceptable Path Control with Aircraft Configuration

characteristics. It was shown (via pilot/vehicle analysis procedures) in Vol. III that path control deficiencies on short final (sink-rate-to-throttle response) also show up in the flare when the throttle is used as a secondary control. Another possible explanation may be that the requirement for a secondary control is unacceptable. This can only be verified by optimizing the secondary control.

The primary and secondary deficiencies for each of the test configurations are summarized in Table 6. Configurations with marginal or unacceptable ratings are seen to have combinations of deficiencies. Many of these limiting deficiencies are not completely independent. That is, low Z_α, low σ_θ, and poor secondary control with throttles all result to some extent from low heave damping, Z_w. The connections between low Z_w and limiting effects for the flare maneuver are summarized below:

TABLE 6

PRIMARY AND SECONDARY DEFICIENCIES FOR EACH OF THE TEST CONFIGURATIONS

CONFIGURATION	ACCEPTABILITY FOR LANDING	PRIMARY DEFICIENCY	SECONDARY DEFICIENCY
BSL1	Marginal to unacceptable; PR: 3-7	Required excessive pitch attitude to flare; low Z_α (see Fig. 9) Moderately large horizontal gust sensitivity compared to level by closed-loop control (Z_u vs. σ_θ in Fig. 10)	Very sluggish secondary control; sink rate to throttle response required 4.6 sec to 1/2 amplitude (see Table 2) Also has mild dynamic coupling (Table 3) but effective thrust inclination angle is not large (61°)
BSL2	Acceptable; PR: 3-3.5		Secondary control not required
BSL2 RLD	Marginal; PR: 4-6	Marginally excessive pitch attitude to flare; marginal Z_α (see (Fig. 9) Moderately large horizontal gust sensitivity compared to level of closed-loop control (Z_u vs. σ_θ in Fig. 10)	Very sluggish secondary control; sink rate to throttle response required 5 sec to 1/2 amplitude
AP1	Unacceptable; PR: 5-8	Required excessive pitch attitude to flare; low Z_α (see Fig. 9) Very low level of closed-loop control capability (low σ_θ)	Sink rate response to secondary control was unacceptable because of dynamic coupling (Table 3) and large effective thrust inclination angle (81°)
AP2	Acceptable; PR: 4-4.5	Large static path/speed coupling could lead to limiting effects in tailwind or tailwind shear (see Fig. 1)	Secondary control not required
AP6	Acceptable; PR: 3-4.5	Same as AP2	Secondary control not required
AP6 RLD	Acceptable; PR: 3-5	Same as AP2	Secondary control not required
AP7	Marginal: PR: 4-6	Marginally excessive pitch attitude to flare; marginal Z_α (see Fig. 9) Moderately large horizontal gust sensitivity compared to level of closed-loop control (Z_u vs. σ_θ in Fig. 10)	Possible deficiencies due to moderate dynamic coupling (Table 3) and moderate effective thrust inclination angle (75°)
AP10	Unacceptable; PR: 6-9	Required excessive pitch attitude to flare; low Z_α Very low level of capability for closed-loop control of sink rate with throttle (low σ_θ)	Sink rate response to secondary control was unacceptable because of dynamic coupling (Table 3) and large effective thrust inclination angle (90°)

- Excessive attitude required for flare (low Z_α):

$$Z_\alpha = U_o Z_w \tag{7}$$

- Low level of closed-loop control capability (low σ_θ):

$$\sigma_\theta \doteq Z_w + \frac{1}{2}\left(\frac{1}{T_E} - \frac{1}{T_F}\right) \tag{8}$$

- Inadequate secondary control due to dynamic coupling; dynamic coupling occurs when:

$$(Z_w - X_u)^2 < |4X_w Z_u| \tag{9}$$

- Inadequate secondary control because of very sluggish sink rate response to throttle:

$$\frac{\dot{h}}{\delta_T} \doteq -\frac{Z_{\delta_T}[s - X_u + (Z_u/\tan\theta_T)]}{(s - X_u)(s - Z_w)} \tag{10}$$

For large thrust inclination angles, θ_T, the response time constant is Z_w.

$$\frac{\dot{h}}{\delta_T} \doteq -\frac{Z_{\delta_T}}{s - Z_w}$$

One final deficiency which did not show up in the simulation, but resulted in significant problems in flight, was adverse steady-state path/speed coupling in a tailwind shear (discussed in Section II-A). In some cases this deficiency resulted in excessive pitch attitudes at flare initiation, leaving nothing left for the flare itself. Like the deficiencies listed above, it also can be attributed to a low value of the heave damping derivative, Z_w. That is, adverse steady-state path/speed coupling occurs when:

$$\tan\theta_T > -\frac{Z_w}{X_w}$$

or, equivalently,

$$\tan\theta_T > \frac{C_{L_\alpha}}{C_L - C_{D_\alpha}} \tag{11}$$

Any of the above factors can result in unacceptable path control (short final or flare and landing). Therefore, a configuration with marginal lift curve slope [recall $Z_w \doteq (\rho S U_o/m) C_{L_\alpha}$] would be suspected of having limiting path control deficiencies. The actual value of Z_w which is limiting depends on its relationship to other key aerodynamic and propulsive parameters according to the relationships established above (Eqs. 7-11). It should be emphasized that the fundamental limitation is on the parameters in Figs. 9 and 10 and on the secondary control characteristics. Low values of Z_w are limiting only in that they adversely affect these parameters (which are related to the basic deficiency in a more comprehensive way).

The landing results may be summarized as follows:

- All of the tested airplanes had a very large engine lag. This made it necessary for the pilots to make attitude primary for landing.
- The pilot ratings for the landing task tended to degrade to unacceptable when:
  - The primary control was in itself marginal (due to low Z_α and/or low σ_θ).
  - Use of the secondary control did not improve the response to the primary control (due to sluggish response or dynamic coupling).
  - The sensitivity to turbulence approached that of a CTOL ($Z_u \doteq -2g/U_o$) (due to low STOL efficiency, η_p).
- Low heave damping, Z_w, was related to most of the limiting deficiencies.
- Excessive pitch attitudes were required for flare when $Z_\alpha < 60$ (ft/sec^2)/rad, necessitating use of throttle as a secondary control.
- None of the configurations which required a secondary control were rated better than marginal. The secondary control characteristics were not separately optimized. Therefore, conclusions regarding the tradeoff between primary and secondary controls for flare and landing cannot be made at this time.

SECTION IV

FLIGHT TEST RESULTS

A. DESCRIPTION OF FLIGHT PROGRAM

The flight test program which spanned a period of about three months was basically a flight version of the final approach and landing task (Task 2.1 on the simulator). The Princeton University Variable Stability NAVION was programmed and checked out to simulate Configurations BSL1 and AP1. The artificial turbulence was identical to that used on the simulator in that a magnetic tape of one hour of the simulator turbulence was used to generate artificial turbulence in flight.

The flight scenario involved the safety pilot's flying the aircraft around the pattern and setting up for each run, with the evaluation pilot taking over on final approach at about 1000 ft. Approach guidance consisted of a 6 deg microwave landing system glide slope and localizer (TALAR) plus a lighting system which provided visual indication of whether the pilot was above or below the 6 deg approach path. The evaluation pilot flew the airplane to touchdown or to the point at which the safety pilot felt an abort was necessary. Each configuration was tested for three basic levels of turbulence and two levels of attitude SAS bandwidth. The levels of turbulence tested were 0, 2.25 ft/sec rms, and 4.5 ft/sec rms. The attitude SAS bandwidth was tested at a basic level of 0.7 rad/sec and also a level of 1.2 rad/sec.

B. FLIGHT RESULTS

The basic NAVION was mechanized with the turbulence tape and several approaches to touchdown were flown with σ_{u_g} = 4.5 ft/sec to gain an appreciation for the level of simulated turbulence with a known airplane. The pilot rating was 4.5, and the pilot commented that the situation appeared to be consistent with tower-reported winds of approximately 15 to 20 kt with gusts to 25 kt. The evaluation pilot noted that the pilot rating for Task 2.1 (final approach and landing) with the basic NAVION in calm air is about 2.5.

This is an important result, because it associates the unreasonably large disturbances in the simulator with STOL response to turbulence rather than with simulation of unrealistically high gusts. Only one pilot flew this portion of the experiment (Princeton project pilot) and only a few approaches and landings were made. Because of its importance, further experimental validation of this result is warranted.

Two levels of attitude SAS were tested: a high-gain SAS and a low-gain SAS. The low-gain SAS resulted in a very sluggish attitude response to column input (3 sec to 75 percent of steady state), whereas the high-gain SAS was quite responsive (1.8 sec to 75 percent). Three levels of turbulence were tested for two configurations (BSL1 and AP1). These configurations were selected because they exhibited marginal characteristics on the simulator and had different limiting effects. That is, BSL1 was very sluggish and AP1 had dynamic coupling problems. The pilot ratings for each of the three levels of turbulence and two levels of SAS response are shown in Table 7 for flare and landing (Task 2.1) and in Table 8 for final approach only.

TABLE 7. COOPER-HARPER RATINGS FOR FLARE AND LANDING (FLIGHT PROGRAM)

TURBULENCE AND SAS	CONFIGURATION BSL1		CONFIGURATION AP1	
	PILOT 1	PILOT 3	PILOT 1	PILOT 3
σ_{u_g} = 0 ft/sec				
High-gain SAS	4.5	4	6.5	5.5
Low-gain SAS	5	5	7	6.5
σ_{u_g} = 2.25 ft/sec			Did not fly enough in turbulence to rate	
High-gain SAS	5	5		6.5
Low-gain SAS	6.5	6		9
σ_{u_g} = 4.5 ft/sec				
High-gain SAS	7	6.5 to 10		10
Low-gain SAS	8	7 to 10		10

TABLE 8. COOPER-HARPER RATINGS FOR FINAL APPROACH (FLIGHT PROGRAM)

TURBULENCE LEVEL σ_{u_g} (ft/sec)	CONFIGURATION BSL1		CONFIGURATION AP1	
	PILOT 1	PILOT 3	PILOT 1	PILOT 3
0	4	4	5.5	5
2.25	5	5.5	—	6.5
4.5	7	8.5 to 10*	—	9 to 10

Ratings did not vary with high and low gain SAS.

*This rating improves to a 6 with increased throttle control power (throttle was limited to ±20% about trim on NAVION).

The following results are indicated from the pilot ratings in Tables 7 and 8.

1. The high-gain pitch attitude SAS resulted in consistently better pilot ratings for landing and had no effect on glide path control (on short final).

2. The turbulence level had a dramatic effect on the ratings with both configurations being clearly unacceptable at $\sigma_{u_g} = 4.5$ ft/sec (Tables 7 and 8).

3. The ratings for maximum turbulence level ($\sigma_{u_g} = 4.5$ ft/sec) were much worse than obtained in the simulation program. For example, comparison of Fig. 8 with Table 7 shows that BSL1 was rated from 3 to 7 on the simulator and from 7 to 10 in flight.

The first of these results is consistent with the closed-loop criterion for landing shown in Fig. 10. That is, σ_θ was increased from 0.51 to 0.76 due to an increase in $1/T_E$ from 0.5 to 1.0 with the "high-gain" SAS.

Result No. 2 is consistent with the simulation in that increasing the turbulence level had a degrading effect on the pilot ratings. This effect was more pronounced in flight, especially for BSL1 on final approach (pilot ratings from 3 to 4.5 in simulation and 6 to 7 in flight). The very poor flight ratings on short final for BSL1 are believed to be a direct consequence of its very sluggish sink-rate-to-throttle response characteristics (see Fig. 2). On this basis we would also expect poor flight ratings for

BSL2 RLD on short final. BSL2 has a higher level of heave damping which would allow the pilots to use pitch attitude to augment the sluggish path response to throttle. The extent to which this is possible is an important consideration for defining minimally acceptable path control. However, testing of secondary control effects was beyond the scope of the present study.

A disparity between simulation and flight (Result No. 3 above) was indicated in that worse pilot ratings were received in flight, even though the peripheral and motion cues were better than in the simulator. It was not possible to resolve the flight/simulator discrepancies (with any confidence) without considerably more testing, which was beyond the scope of this program. There are two possible hypotheses which help to "explain" the data. These are summarized below.

1. The rating effect of the 4.5 ft/sec turbulence is more pronounced for flight than for simulation. To some extent this may be due to the fact that during the simulation many of the landing problems were attributed to poor simulator cues. The flight tests served to illustrate that the much improved visual and motion cues in flight were of <u>no help</u> in regulating against the large gust inputs near touchdown. In fact, the improved sink rate cues served to increase the pilot's awareness of "how bad things really were." Sink rates of 1200 to 1400 ft/min on short final tend to be far more dramatic in the flight environment than on the simulator with the Redifon display.

2. There were certain discrepancies in the environmental, task, and procedural variables between flight and simulation.

A very short (two-day) post-flight simulation (conducted by NASA Ames on the FSAA) was undertaken as a quick look at the problem. The simulation was divided into two phases, as follows.

<u>Phase I — Direct simulator/flight comparison</u>

1. The simulator was programmed to abort (go into reset mode) if the sink rate exceeded approximately 6.5 ft/sec below an altitude of about 10 ft. This criterion was based on examination of the flight test strip chart records which showed consistent safety pilot behavior in this regard.

2. Physical stops were clamped on the FSAA simulator throttle quadrant which limited thrust excursions about trim to ±20 percent (NAVION control power was 20 percent of simulated STOL).

3. The pilot position was set to simulate the NAVION (eye height of 8 ft and longitudinal pilot position at the center of gravity).

4. Engine noise was eliminated. (There are no correlatable changes in sound with changes in power in the NAVION since thrust is varied via a beta prop at constant engine rpm).

Phase II — Same scenario as pre-flight simulation

1. Assume gear is "strong as required within reason," i.e., no abort.

2. The throttle stops were removed.

3. Engine noise cues were turned back on.

4. Pilot position was made consistent with a large aircraft (eye height 17 ft and 20 ft forward of the aircraft center of gravity).

The pilots both commended that subjectively the large shears had the same effect in the simulator as in flight, e.g., they appeared extreme. A summary of the pilot ratings for each phase is shown in Table 9. These ratings

TABLE 9. COOPER-HARPER RATINGS FOR FLARE AND LANDING POST-FLIGHT SIMULATION — CONFIGURATION BSL 1

TURBULENCE LEVEL σ_{u_g} (ft/sec)	PHASE	FLARE AND LANDING		FINAL APPROACH	
		PILOT 1	PILOT 3	PILOT 1	PILOT 3
0	I	4.5	4	3	4
2.25	I	5.5	4 to 4.5	4	5
4.5	I	7	5.5 to 10	5	7
0	II	3	4	3	4
2.25	II	3.5	4.5 to 5	4	5
4.5	II	5	6 to 10	5	7

are closer to the flight values than the original simulation, perhaps lending some credence to hypothesis No. 1 above (since both pilots had recent flight experience). Pilot 1 felt that the differences between Phase I and Phase II (effect of experimental variables) were significant (about two rating points), and Pilot 3 did not (ratings about the same). Clearly, more data would be required to resolve hypothesis No. 2 on page 34.

While the simulator results did not agree well with flight in terms of absolute value of pilot ratings, the problem areas identified via pilot commentary were identical. Since the objective of this program was to find effects or combinations of effects which are limiting, the pilot rating discrepancies do not detract from the simulation results. However, these discrepancies should be resolved before actual numerical boundaries are derived for certification criteria.

One final comment: the majority of simulation was done on the S-16 simulator (very limited motion and marginal Redifon), whereas the post-flight simulation was done on the FSAA (better motion and visual). A three-day exercise was undertaken during the original simulation where three pilots flew Configurations AP7 and AP10 on the FSAA and S-16 back to back. The FSAA ratings were one to two points <u>better</u> than the S-16, e.g., in the wrong direction to resolve the simulator/flight discrepancy.

SECTION V

SUMMARY OF CONCLUSIONS

- Flight path control deficiencies were most apparent during the final portion of the approach and during the flare and landing. Vehicle deficiencies were not apparent when further out on the approach despite the fact that the pilots were in IFR conditions, e.g., being "close in" was more critical than being on instruments.

- Two characteristic deficiencies resulted in unacceptable flight path control on short final. These were:

  1. A near vertical thrust inclination angle combined with dynamic coupling. Dynamic coupling occurs when $(Z_w - X_u)^2 < -4Z_wX_u$.

  2. An overly sluggish sink-rate-to-throttle response. This characteristic has been identified in terms of time to 1/2 amplitude of the sink rate to a throttle step in Ref. 7. There were indications of this deficiency with BSL1 in flight but not in the simulation.

- Exact boundaries where the above two deficiencies become unacceptable cannot be identified at this time. However, dynamic coupling combined with thrust inclination angles over 81 deg is a conservative estimate based on the simulation results for AP1. Likewise, a time to 1/2 amplitude for the sink rate response to a step throttle of 4.5 sec was found to be limiting in the flight program (based on BSL1 results). This is somewhat greater than the limiting value of 3 sec defined in Ref. 7. It is suspected that this value depends on the ability to use pitch attitude to augment path control with throttle.

- The pilot ratings were noticeably more critical for a given configuration in flight than in the simulation program. Determination of the reasons for this discrepancy was beyond the scope of the present program.

- Low heave damping, Z_w, was related to most of the limiting deficiencies for flight path control and the flare and landing.

- Excessive pitch attitudes were required for the flare when $Z_\alpha < 60$, necessitating the use of throttle as a secondary control.

- The turbulence level had a significant degrading effect on the pilot ratings for final approach and landing with large low frequency horizontal gusts (wind shears) being the major contributor.

- The pilots noted that the large low frequency effects of the turbulence model seemed extreme in the simulator. Two pilots flew the same turbulence tape in the Variable Stability NAVION and felt the effects were subjectively the same as in simulation for the tested powered-lift configuration. One pilot flew the same turbulence tape in the unmodified Variable Stability NAVION (all feedback gains turned to zero) and rated the final approach and landing as a 4.5. Hence, there is evidence that: 1) the simulated turbulence was not excessively large; and 2) the simulator did not magnify the effect of turbulence.

- Static coupling between flight path and airspeed was not found to result in significant problems unless it resulted in decreased safety or performance margins.

- It was not possible to decouple the path and speed responses by means of a flight director. The flight director was effective only when the speed command (pitch bar) was utilized as a low frequency trim function.

- The averaged rms glide slope tracking performance was reduced 25 to 40 percent with the flight director. The lateral director resulted in an 86 percent reduction in rms tracking error.

REFERENCES

1. Heffley, Robert K., Robert L. Stapleford, and Robert C. Rumold, Airworthiness Criteria Development for Powered-Lift Aircraft — A Program Summary, Systems Technology, Inc., Tech. Rept. 1047-4, forthcoming.

2. McRuer, Duane, Dunstan Graham, et al., Human Pilot Dynamics in Compensatory Systems — Theory, Models and Experiments with Controlled Element and Forcing Function Variations, AFFDL-TR-65-15, July 1965.

3. Craig, Samuel J., Irving L. Ashkenas, and Robert K. Heffley, Pilot Background and Vehicle Parameters Governing Control Technique in STOL Approach Situations, FAA-RD-72-69, June 1972.

4. Franklin, James A., and Robert C. Innis, "Flight-Path and Airspeed Control for the STOL Approach and Landing," STOL Technology, NASA SP-320, Oct. 1972, pp. 181-198.

5. Heffley, Robert K., and Robert L. Stapleford, A STOL Airworthiness Investigation Using a Simulation of an Augmentor Wing Transport. Vol. I: Summary of Results and Airworthiness Implications, FAA-RD-74-179-I, Mar. 1974; and Robert K. Heffley, Robert L. Stapleford, et al., Vol. II: Simulation Data and Analysis, FAA-RD-74-179-II, Oct. 1974. (Also, NASA TM X-62,395 and TM X-62, 396).

6. Hoh, Roger H., Richard H. Klein, and Walter A. Johnson, Design of a Flight Director/Configuration Management System for Piloted STOL Approaches, NASA CR-114688, Sept. 1973.

7. Heffley, Robert K., John M. Lehman, et al., A Simulator Evaluation of Tentative STOL Airworthiness Criteria. Vol. I: Simulation Results and Analysis. Vol. II: Background Information, Systems Technology, Inc., Tech. Rept. 1047-3-I and 1047-3-II, June 1975.